Cdc42 GTPase-activating protein deficiency promotes genomic instability and premature aging-like phenotypes

Lei Wang, Linda Yang, Marcella Debidda, David Witte, and Yi Zheng*

Divisions of Experimental Hematology and Pathology, Molecular Developmental Biology Graduate Program, Children's Hospital Research Foundation, University of Cincinnati, Cincinnati, OH 45229

Edited by Frederick W. Alt, Harvard Medical School, Boston, MA, and approved November 28, 2006 (received for review October 16, 2006)

Cdc42 is a member of the Rho GTPase family known to regulate cell actin cytoskeleton organization, polarity, and growth, but its function in mammalian organismal physiology remains unclear. We found that natural aging of WT mice is marked with increased Cdc42 activity in various tissues. Among the negative regulators of Cdc42, gene targeting of Cdc42 GTPase-activating protein (Cdc42GAP) results in constitutively elevated Cdc42-GTP level in diverse tissues of adult mice; significantly shortened life span of the animals; and multiple premature aging-like phenotypes, including a reduction in body mass, a loss of subdermal adipose tissue, severe lordokyphosis, muscle atrophy, osteoporosis, and reduction of reepithelialization ability in wound-healing. Cdc42GAP$^{-/-}$ mouse embryonic fibroblasts and/or tissues display reduced population doubling, significantly dampened DNA damage repair activity after DNA-damaging agent treatment, accumulated genomic abnormalities, and induction of p53, p16^{Ink4a}, p21^{Cip1}, and senescence-associated β-galactosidase expressions. Furthermore, Cdc42 activation is sufficient to promote a premature cellular senescence phenotype that depends on p53. These results suggest a role of Cdc42 activity in regulating mammalian genomic stability and aging-related physiology.

cell senescence | DNA damage repair | genomic stability | Rho GTPases

Cdc42 is a member of the Rho GTPase family known to regulate multiple eukaryotic cell functions, including actin cytoskeleton reorganization, polarity establishment, and cell growth (1–3). Like other members of the Rho family, Cdc42 cycles between the inactive, GDP-bound state and the active, GTP-bound state in cells and is tightly controlled by a number of regulators under physiologic conditions. The current biochemical model depicts that, upon ligand binding to cell surface receptors or in response to cellular stress, Cdc42 can be activated to recognize specific downstream effectors to mediate multifacet cell functions. To date, however, most studies of Cdc42 function in mammalian cells have been carried out by forced expression of dominant-negative or active Cdc42 mutants in clonal cell lines, because conventional gene targeting of Cdc42 in mice led to embryonic lethality at embryonic day 7.5, hindering the effort to study Cdc42 function in mammalian physiology (4).

Cdc42 GTPase-activating protein (Cdc42GAP; also known as p50RhoGAP or ARHGAP1) is a ubiquitously expressed negative regulator of Cdc42 that catalyzes GTP hydrolysis by Cdc42, leading to Cdc42 inactivation (5). Gene targeting of Cdc42GAP in mice produces a Cdc42 gain-of-activity mouse model that phenotypically displays decreased cell number and increased basal apoptosis during the perinatal period (6). Characterization of the survived adult mice of this gain-of-activity mouse model leads to the findings reported here that Cdc42GAP plays an important role in regulating mammalian cell genomic stability. The Cdc42GAP knockout primary cells show reduced DNA damage repair ability; increased genomic abnormalities; induction of multiple cell cycle inhibitors, including p53 and p16^{Ink4a}; and premature senescence. These effects may be reflected in animal physiology as a cohort of early aging-like phenotypes. Our results present an interesting possibility linking Cdc42 activity to genome maintenance, cellular senescence regulation, and mammalian aging.

Results and Discussion

In mammalian systems, Cdc42 activity has been shown to be important in regulating skin stem/progenitor cell differentiation into hair follicle cells, controlling neuroepithelial stem/progenitor polarity and brain hemispheric bifurcation, and regulating cell number and growth during the perinatal development period (6–9). Interestingly, an examination of Cdc42 activity in WT adult mice of various ages reveals that the relative Cdc42-GTP level of older animals is significantly higher than that of younger ones in diverse tissues, including heart, brain, lung, liver, bone marrow, spleen, and kidney (Fig. 1*A* and data not shown), raising the possibility that increased Cdc42 activity is involved in the normal aging process.

To determine whether the increased Cdc42 activity associated with natural aging may have physiological relevance, we examined the Cdc42 negative regulator, Cdc42GAP, in gene-targeted mice after they have reached adulthood. Previous studies of the homozygous Cdc42GAP knockout mice during the perinatal period indicated that various tissues/cells contained elevated Cdc42-GTP, and the embryos/new born pups of the Cdc42GAP$^{-/-}$ genotype displayed reduced organ/organismal size that are related to increased spontaneous apoptosis in various cell types (6). In adult Cdc42GAP$^{-/-}$ mice, Cdc42 activity was constitutively higher in multiple tissue/cell types than that of the matching WT mice, whereas the level of RhoA-GTP or Rac1-GTP remained similar to that of WT (Fig. 1*B*; data not shown), suggesting a specific gain-of-Cdc42 activity in the adult animals similar to that during the perinatal period. The majority of Cdc42GAP$^{-/-}$ mice died during the neonatal period due to their smaller size and weak physique (6). However, a proportion of them (≈7%) could survive the neonatal period under foster care by unrelated nurturing females. Despite regular milk intake and normal serum glucose and insulin concentrations found in the homozygous mice in the postnatal period [supporting information (SI) Fig. 6], weight gain of Cdc42GAP$^{-/-}$ mice started to decelerate at ≈3 months of age compared with ≈5 months of age for WT or heterozygous mice, and the mature homozygotes were ≈30% reduced in body weight due to a decrease in overall cellularity (Fig. 1*C* and data not shown). The median life

Author contributions: L.W. and Y.Z. designed research; L.W., L.Y., M.D., D.W., and Y.Z. performed research; L.W., L.Y., and Y.Z. contributed new reagents/analytic tools; L.W., L.Y., D.W., and Y.Z. analyzed data; and L.W. and Y.Z. wrote the paper.

The authors declare no conflict of interest.

This article is a PNAS direct submission.

Abbreviations: GAP, GTPase-activating protein; MEF, mouse embryonic fibroblast; ROS, reactive oxygen species; SA-β-gal, senescence-associated β-galactosidase.

*To whom correspondence should be addressed at: Division of Experimental Hematology, Children's Hospital Research Foundation, 3333 Burnet Avenue, Cincinnati, OH 45229. E-mail: yi.zheng@cchmc.org.

This article contains supporting information online at www.pnas.org/cgi/content/full/0609149104/DC1.

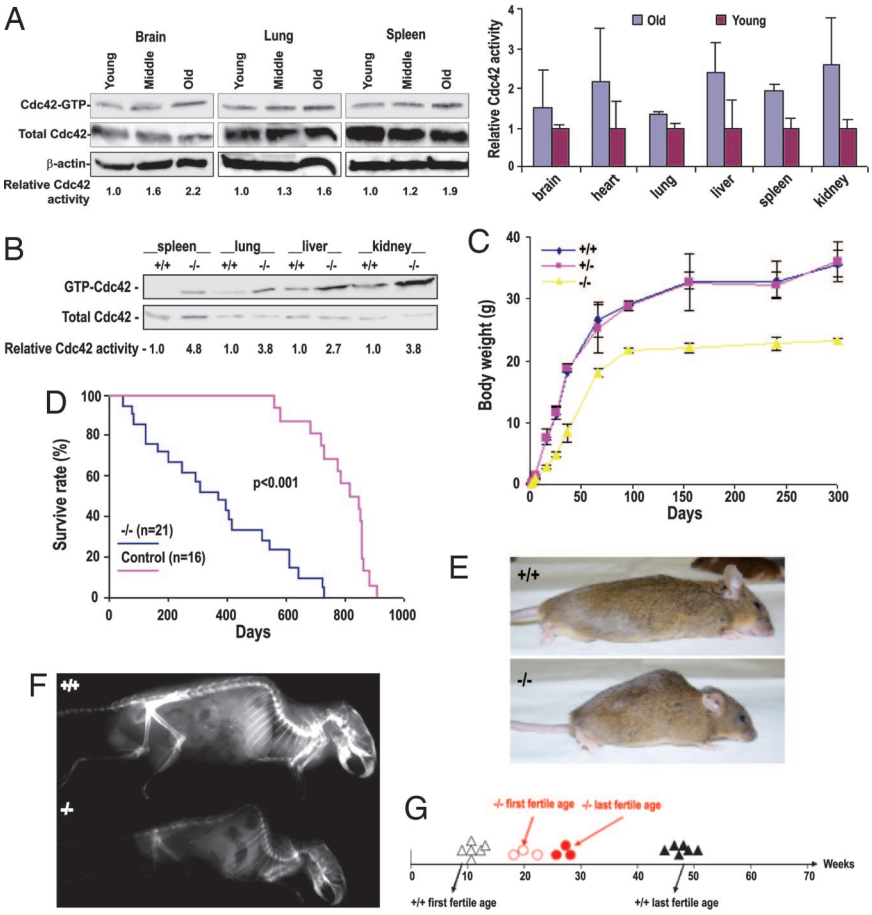

Fig. 1. Increased Cdc42 activity in the course of natural aging in mice and the effects of Cdc42GAP gene targeting on the growth, bone structure, life span, and fertility period of adult mice. (*A*) Normal aging in mice is associated with increased Cdc42 activity. (*Left*) The Cdc42-GTP levels of various tissues from young (2-month-old), middle-aged (12-month-old), and elderly (24-month-old) mice were examined by GST-PAK1 effector domain pull-down assays. A representative blot from two experiments is shown with densitometry quantifications. (*Right*) The Cdc42-GTP levels of different tissues from 1.5-month-old (Young) and 26-month-old (Old) WT mice were examined by the effector pull-down assay. The quantifications were obtained from three independent experiments. (*B*) Different organs from 8-month-old mice were lysed with sonication. The lysates were subjected to GST-PAK1 effector pull-down, and the bound proteins were immunoblotted by a monoclonal anti-Cdc42 antibody. One set of data from two repeated experiments is shown. The underlining numbers indicate relative Cdc42-GTP quantified by densitometry scanning. (*C*) Body weights of 20 mice in each group ($Cdc42GAP^{+/+}$, $Cdc42GAP^{+/-}$, and $Cdc42GAP^{-/-}$) tracked with increasing age. (*D*) Survival curves of 16 control ($Cdc42GAP^{+/+}$ and $Cdc42GAP^{+/-}$) and 21 $Cdc42GAP^{-/-}$ mice. The median life spans were 12 and 27 months for $Cdc42GAP^{-/-}$ and control mice, respectively. (*E*) Photographs of representative 12-month-old live $Cdc42GAP^{+/+}$ and $Cdc42GAP^{-/-}$ males. The $Cdc42GAP^{-/-}$ mouse shows reduced size and severe lordokyphosis. (*F*) X-rays of representative 15-month-old male mice showing skeletal changes with severe lordokyphosis in the $Cdc42GAP^{-/-}$ mouse. (*G*) Delayed, reduced, and shortened reproductive period in the $Cdc42GAP^{-/-}$ female mice.

span of the $Cdc42GAP^{-/-}$ mice was ≈12 months, whereas the control (WT or heterozygous) mice remained vital until a median age of ≈27 months (Fig. 1*D*). The survival curve of the homozygous mice is somewhat different from the typical Gompertz curve but is similar to those reported for BubR1 (a mitotic checkpoint regulator) knockout (10) or p44 (a short isoform of the p53 tumor suppressor) transgenic (11) animals. Kyphosis and lack of vigor in $Cdc42GAP^{-/-}$ mice became evident at the age of ≈12 months (Fig. 1*E*). Skinned $Cdc42GAP^{-/-}$ mice at 15 months of age showed a clear reduction in body mass, a substantial loss of subdermal adipose tissue, severe lordokyphosis, and muscle atrophy (data not shown). An x-ray scan showed a significant kyphosis phenotype and reduced bone mineral density (BMD) in $Cdc42GAP^{-/-}$ mice at the age of 15-month (Fig. 1*F*). Further quantification of the dissected bones of $Cdc42GAP^{-/-}$ mice revealed 3- and 2.6-fold reductions of BMD in the tibia and femur, respectively (SI Fig. 7). In addition, both male and female $Cdc42GAP^{-/-}$ mice lost fertility at an earlier age compared with that of WT. In mating between $Cdc42GAP^{-/-}$ females and WT males, the homozygotes became infertile at 26 weeks old compared with 48 weeks old for WT (Fig. 1*G*). These observations indicate that Cdc42GAP deficiency results in the constitutively elevated Cdc42-GTP level, reduced body size, early kyphosis, reduced BMD, shortened fertility period, and reduced life span in adult mice.

The H&E stained sections through the 8-month-old female mouse vertebral body showed that the $Cdc42GAP^{-/-}$ mice had a thinner, bowed cortex and thinner trabeculae compared with WT mice (Fig. 2*A*). Similarly, the longitude sections of the femur of the homozygous mice showed a reduction of cortical bone thickness compared with that of WT mice (data not shown). These observations are in agreement with the gross appearance and clinical features of osteoporosis. The spleen, liver, and kidneys of adult $Cdc42GAP^{-/-}$ mice were reduced in mass due to a decrease in overall cellularity, which was evident in the H&E-stained sections of the spleen, and the T and B cell-containing white pulp regions of 12-month-old $Cdc42GAP^{-/-}$ spleen were markedly reduced compared with those of age-matched WT mice (Fig. 2*B* and data not shown), suggesting pronounced lymphoid atrophy in the homozygotes. Consistent with the apparent reduction of subdermal adipose tissue, histological analysis of the cross-sections of dorsal skin revealed an almost complete absence of s.c. adipose cells in 9-month-old $Cdc42GAP^{-/-}$ mice (Fig. 2*C*). A loss in muscle mass and muscle atrophy were also confirmed by the examination of H&E-stained skeletal muscle sections from 12-month-old $Cdc42GAP^{-/-}$ mice and the age-matched WT mice (Fig. 2*C*). The $Cdc42GAP^{-/-}$ mice also showed marked reduction in hair regeneration after removal of the dorsal hair by shaving, whereas the age- and sex-matched WT displayed robust hair regrowth (SI Fig. 8). The ability to tolerate stresses, such as wound healing, an aging-associated activity (12) of the $Cdc42GAP^{-/-}$ mice, was significantly reduced compared with that of WT (Fig. 2*D*). Histopathological analysis of the wound sections showed little reepithelialization in the wound edge of the $Cdc42GAP^{-/-}$ mice, whereas complete reepithelialization of WT mice was evident 4 days after the wound was introduced (Fig. 2*E*). In addition to these observations, a number of hematopoietic phenotypes of the homozygous mice, including anemia, reduced spleen and bone marrow cellularities, defects of hematopoietic stem cell engraftment to the bone marrow, and increased sensitivity of hematopoietic stem cells to induced mobilization (13, 14) were consistent with early aging in the hematopoietic system. Importantly, an examination of young homozygous mice (<4 month old) before the manifestation of obvious

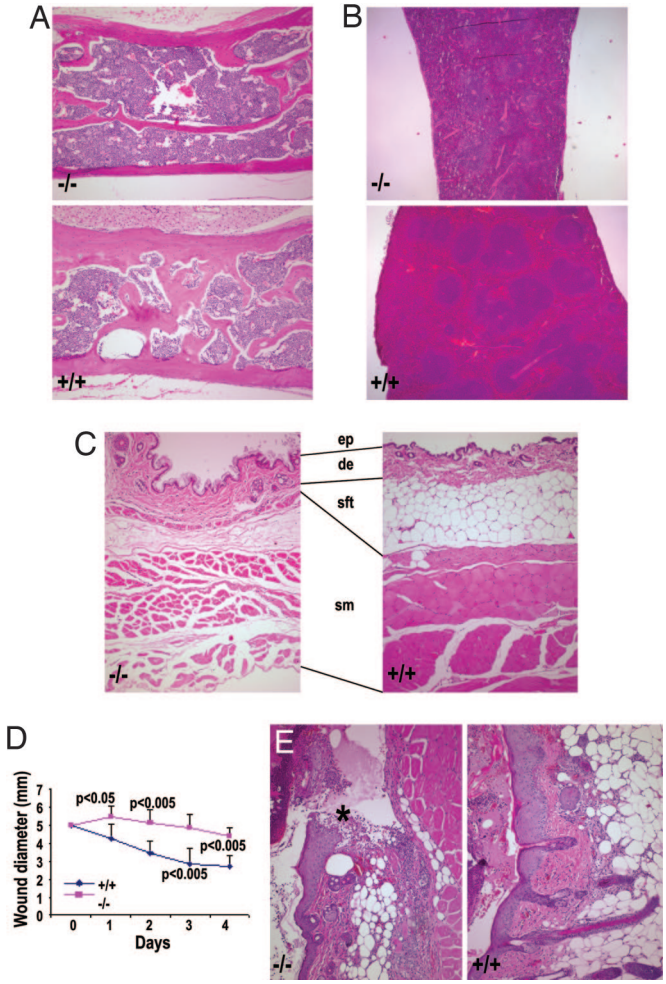

Fig. 2. Cdc42GAP$^{-/-}$ mice display premature aging-like phenotypes in various tissues. (*A*) H&E sections of 8-month-old female homozygous or WT mouse vertebral bodies. The Cdc42GAP$^{-/-}$ mouse shows a thin, bowed cortex and thin trabeculae in contrast with the WT mouse. (*B*) H&E sections of 12-month-old female mouse spleens. The Cdc42GAP-deficient mouse shows decreased volume in the white pulp and red pulp of the spleen and smaller lymphoid follicles and decreased red blood cells on the sinusoids of the red pulp. (*C*) H&E staining of 9-month-old female mouse dorsal skin sections. In the Cdc42GAP$^{-/-}$ mouse, the s.c. layer is completely collapsed due to the loss of adipocytes, and the muscle layer shows atrophy at the muscle fibers compared with the WT control. Ep, epidermis; de, dermis; sft, s.c. fat tissue; sm, skeletal muscle. (*D*) Wound healing ability compared in 8-month-old female mice. (*E*) H&E staining of a skin wound 4 days after wounding. The WT shows complete epithelialization of the wound, whereas there is no closure at the wound (indicated by asterisk) in the Cdc42GAP-deficient mouse. The experiments were repeated at least twice, and one set of representative data is shown.

phenotypes revealed no major abnormalities in the bone, skin, and spleen (SI Fig. 9 *A* and *B* and data not shown), suggesting that the aging-like phenotypes of the Cdc42GAP$^{-/-}$ mice are not due to an early developmental disorder. Furthermore, a number of phenotypes of the homozygous mice, including reduced cortical bone thickness, kyphosis, and loss of muscle mass and epidermal tissues, could be found in the old (>2.5 years old) WT mice (SI Fig. 9 *C* and *D* and data not shown). As summarized in SI Table 1, collectively these results provide strong evidence that Cdc42GAP deficiency causes premature aging-like phenotypes in the animals.

Staining of the tissues of 9-month-old adults, including liver, kidney, and spleen, for senescence-associated β-galactosidase (SA-β-gal) revealed a strong activity of this senescence marker in the homozygous mice that was not detectable in the tissues of age- and sex-matched WT mice (Fig. 3*A* and SI Fig. 10), indicating that Cdc42GAP$^{-/-}$ adult tissues may undergo premature senescence. Interestingly, increased apoptosis of the homozygous tissues observed during the perinatal period was absent in the adult homozygotes when the elevated SA-β-gal activity was evident (ref. 6 and data not shown). Cdc42GAP$^{-/-}$ mouse embryonic fibroblast (MEF) cells, which contain ≈3-fold higher Cdc42-GTP but normal Rac1-GTP or RhoA-GTP contents compared with WT MEF cells (6), exhibited significantly increased SA-β-gal activity and accumulated a flattened and enlarged senescent morphology beginning at passage 6 when WT MEF cells were negative for SA-β-gal activity and were contractual in morphology (Figs. 3*B* and SI Fig. 11). The Cdc42GAP$^{-/-}$ MEF cells started to decelerate in growth at passages 5–7 when the matched WT MEF cells were growing exponentially (Fig. 3*C*) (6), and they underwent massive replicative senescence after passage 7, whereas most WT MEF cells did not reach senescence until passage 13 (SI Fig. 11 and data not shown). In addition, a significantly higher percentage of Cdc42GAP$^{-/-}$ MEF cells at passage 7 formed larger foci in the nucleus than WT cells (SI Fig. 12). These results indicate that Cdc42GAP deficiency induces early tissue/cell senescence.

One well recognized contributing factor to mammalian premature aging and cell senescence is increased genomic instability (15). Metaphase spreading analysis showed that >30% primary splenocytes from 8-month-old homozygous mice were aneuploid, whereas age- and sex-matched WT splenocytes had no detectable aneuploidy (Fig. 3*D*), indicating that the Cdc42GAP$^{-/-}$ tissue suffered genomic instability. In support of this finding, Cdc42GAP$^{-/-}$ MEF cells showed a significant increase of double nuclei cells under DAPI staining compared with WT cells at passage 7 (SI Fig. 12). Karyotype analysis of the later passages of MEF cells (passage 6–7) further revealed that, although most chromosomes from WT cells (≈80%) remained intact, 42% of Cdc42GAP$^{-/-}$ cells contained at least one chromosome aberration, 20% contained two or more aberrations, and 14% contained three or more aberrations (Fig. 3*E*). The percentage and the degree of aneuploidy also significantly increased in Cdc42GAP$^{-/-}$ MEF cells, with >32% of cells displaying abnormal chromosome numbers ranging from 72 to 102, whereas most WT cells were diploid (Fig. 3*E* and SI Fig. 13). Karyotype analysis of the chromosomal damages indicates that the aberrations of the homozygous MEF cells were diverse, including chromatid break, premature sister chromatid separation (a hallmark of a defective spindle assembly checkpoint), translocation, chromosome breaks, dicentric chromosome, and chromosome fragmentation (Fig. 3*F* and SI Table 2), suggesting that the DNA damage repair machinery is compromised in Cdc42GAP$^{-/-}$ cells. Immunofluorescence staining of phospho-H_2AX in the cell nucleus, a DNA damage response marker (16), shows that, although 10% of passage 7 Cdc42GAP$^{-/-}$ MEF cells were positive for the DNA damage marker, <1% of WT cells were positive (Fig. 3*G*). The correlation between the onset and progression of the aging-like phenotypes of the Cdc42GAP$^{-/-}$ mice and the observed degree and severity of the genomic aberrations in Cdc42GAP$^{-/-}$ cells supports a role of Cdc42 in the development of the progeroid features.

To determine the possible mechanism of the accumulated DNA damages in Cdc42GAP$^{-/-}$ cells, we compared the endogenous reactive oxygen species (ROS) level of the homozygous cells with that of WT cells, because Rac1 and Rac2, two closely related Rho GTPases, are known regulators of cellular ROS (17). SI Fig. 14 shows that Cdc42GAP$^{-/-}$ cells displayed a ROS activity similar to that of WT cells, indicating that Cdc42GAP regulates genomic stability through an endogenous ROS-independent mechanism. Because of the similarities of multiple Cdc42GAP$^{-/-}$ mouse phenotypes to those of a number of gene targeted mouse models of DNA damage repair molecules, including the Brca1$^{-/-}$p53$^{+/-}$, Ku80$^{-/-}$, and Mtr$^{-/-}$Wrn mouse models (12, 18, 19), we further probed the responsiveness of the early passaged Cdc42GAP$^{-/-}$

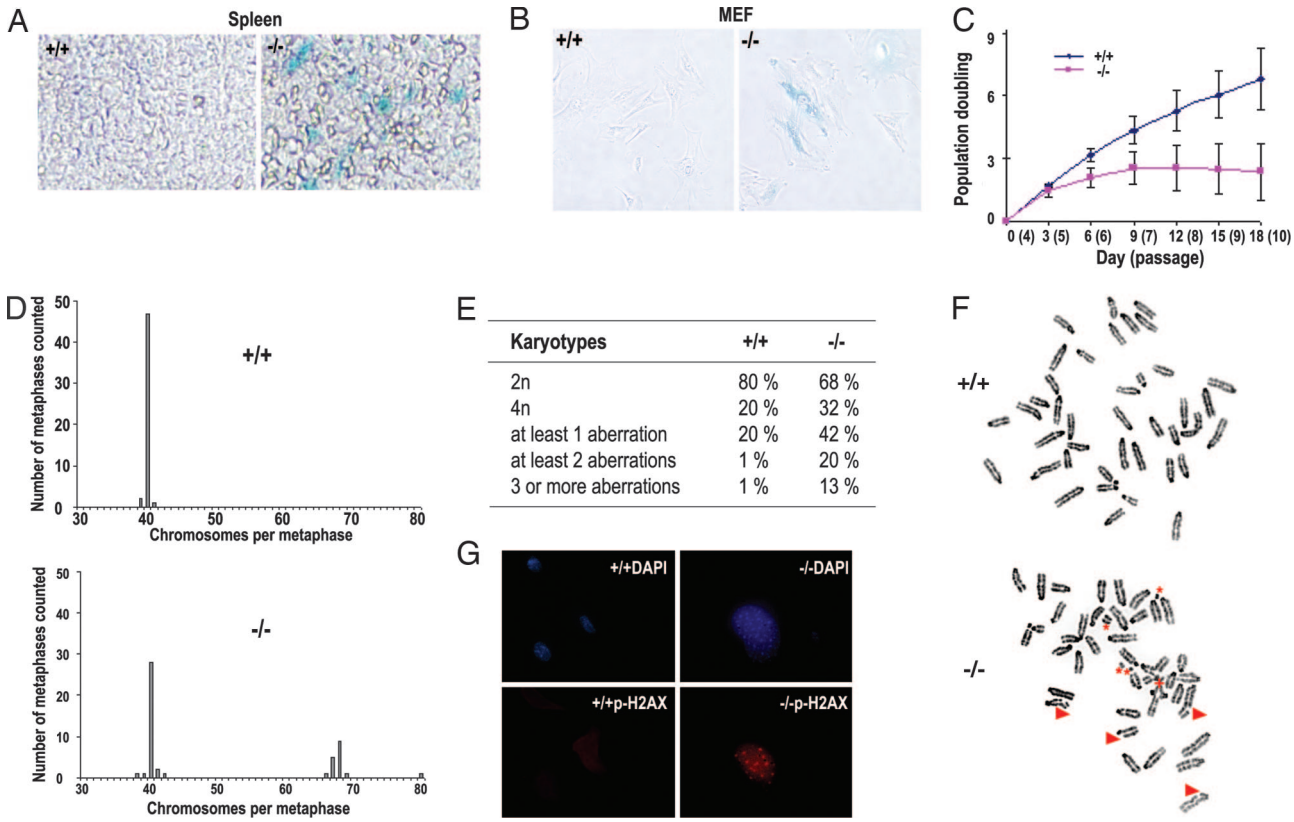

Karyotypes	+/+	-/-
2n	80 %	68 %
4n	20 %	32 %
at least 1 aberration	20 %	42 %
at least 2 aberrations	1 %	20 %
3 or more aberrations	1 %	13 %

Fig. 3. Cdc42GAP$^{-/-}$ cells undergo early senescence and show increased genomic instability. (*A* and *B*) SA-β-gal activities in the spleen sections of 9-month-old female mice (*A*) and passage-6 MEF cells (*B*). The mutant MEF cells show a flattened and enlarged morphology that is associated with β-galactosidase staining. (*C*) MEF cells (passage 4) were replated at a density of 1×10^6 per 10-cm culture dish every 3 days, and the population doubling times were derived. (*D*) Metaphase spreading profiles of 50 splenocytes from 8-month-old female WT and homozygous mice. (*E*) Passage-6 MEF cells were subjected to karyotype analysis, and the chromosome abnormalities are summarized. (*F*) A set of representative pictures of chromosome structures are shown for both genotypes. Arrowheads point to the chromatid breaks, asterisks indicate chromosome fragments, and the plus sign indicates a fusion and complex rearrangement. (*G*) Passage-7 MEF cells were stained with anti-*p*-H_2AX antibody and DAPI to reveal cell nucleus and DNA-damage foci. Three independent pairs of MEF cells were examined, and the pairs behaved similarly.

cells to various DNA damage agents. In the DNA damage response growth assay, the Cdc42GAP-deficient cells showed a broad defect of DNA damage repair activity (Fig. 4), which manifested as significantly higher percentages of cell death among the homozygous cells compared with WT cells after treatment by increasing doses of H_2O_2, ionizing irradiation, camptothecin, methyl-methane sulfonate, or mitomycin C. Thus, the accumulated diverse genomic abnormalities found in the later passages of Cdc42GAP$^{-/-}$ cells may be attributable, at least in part, to impaired DNA damage repair activities.

A consequence of sustained genomic damage in the cells is the induction of multiple DNA-damage-response and/or senescence genes (20, 21). The expressions of p53, p21^{Cip1}, p16^{Ink4a}, and phospho-p53 (Ser-15) in Cdc42GAP$^{-/-}$ MEF cells were significantly higher than those of WT MEF cells after similar passages, whereas p19^{ARF} in the homozygous cells showed a similar trend of increase with passages, like the WT cells (Fig. 5*A*). The protein levels of p53, p21^{Cip1}, p16^{Ink4a}, phospho-p53 (Ser-15), and the DNA damage marker phospho-H_2AX in Cdc42GAP$^{-/-}$ tissues from 8-month-old mice were also significantly higher than those in the corresponding tissues of matched WT mice (Fig. 5*B*). These results provide evidence that activation of the p53-regulated pathway, p21^{Cip1} and p16^{Ink4a} in particular, is associated with Cdc42GAP-deficiency-induced early senescence. To examine the question of whether elevated Cdc42 activity in the Cdc42GAP-deficient cells is sufficient to account for the early senescence phenotype, we expressed an activating mutant of Cdc42, Cdc42F28L, in primary WT MEF cells and assayed for the SA-β-gal activity of the cells in comparison with that of matching EGFP-expressing cells at different passages. Cdc42F28L expression caused a significant increase in SA-β-gal-positive cell population (35% in Cdc42F28L cells compared with 7% in EGFP-expressing cells) in early passaged MEF cells (Fig. 5*C*), indicating that Cdc42 activation is sufficient for the induction of early cell senescence.

To further explore the possibility that the senescence phenotype of Cdc42GAP$^{-/-}$ cells might be rescued by a p53 defect, we generated Cdc42GAP$^{+/-}$p53$^{+/-}$ mice and attempted to prepare MEF cells from the crossbred. Of 44 embryos, six with the Cdc42GAP$^{-/-}$p53$^{+/-}$ genotype and none of the Cdc42GAP$^{-/-}$ p53$^{-/-}$ genotype were obtained. The Cdc42GAP$^{-/-}$p53$^{+/-}$ MEF cells grew at a rate between that of p53$^{+/-}$ and WT cells and showed a basal senescent population comparable with that of p53$^{+/-}$ or WT cells at passage 7, whereas the p53$^{-/-}$ and Cdc42GAP$^{-/-}$ MEF cells proliferated with a linear curve and a bend-population doubling curve and were senescence-resistant and senescence-prone at similar passages, respectively (Fig. 5 *D* and *E*). These results indicate that Cdc42 activation-induced premature senescence depends on p53.

The limited life span of cells and animals may result from replicative senescence in response to various stresses, including DNA damage (22), telomere erosion (23), ROS (24), and/or inappropriately activated oncogenes (25). The Cdc42GAP$^{-/-}$ mice present a gain-of-Cdc42-activity animal model that mimics mitogenic signal-induced Cdc42 activation (6) and allow an assessment of the possible effects of Cdc42 activation on animal and cell physiology. We demonstrate that Cdc42GAP deficiency causes the

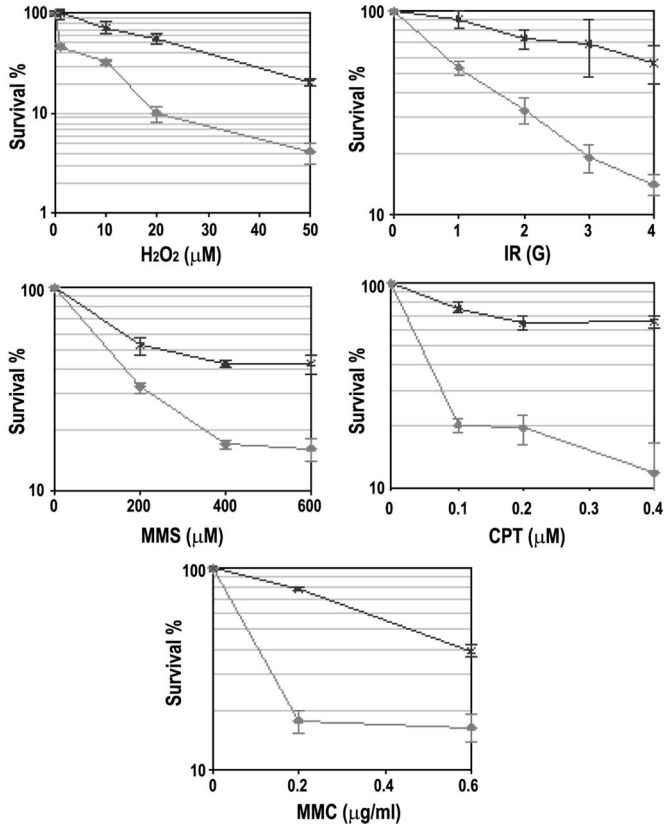

Fig. 4. Impaired DNA damage repair ability of Cdc42GAP-deficient MEF cells after treatment with various DNA-damaging agents. MEF cells of early passages were treated with the indicated doses of IR, H_2O_2, camptothecin (CPT), methyl-methane sulfonate (MMS), or mitomycin C (MMC), and the surviving cell numbers under each condition were quantified after 7 days. The survival rates were normalized to those of the nontreated cells.

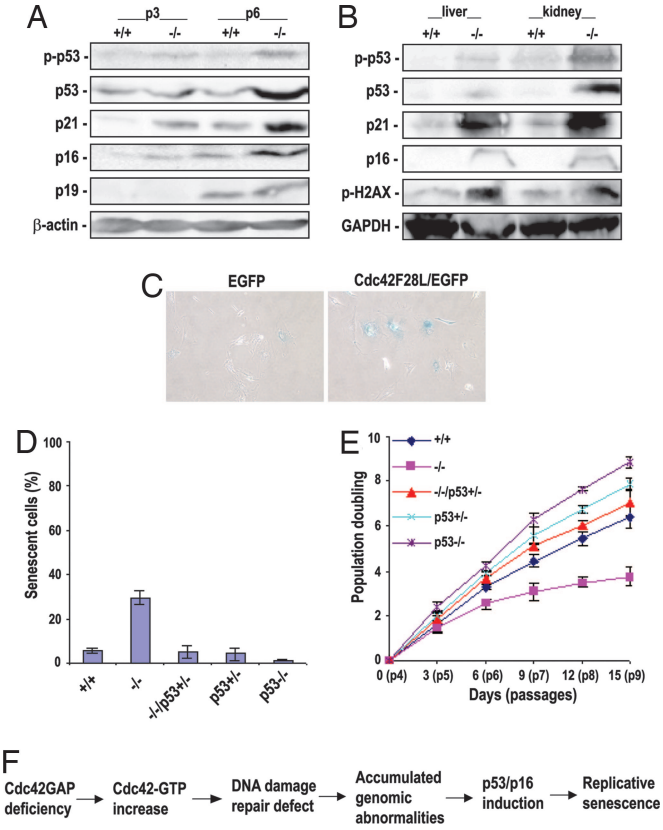

Fig. 5. The early senescence of Cdc42GAP$^{-/-}$ cells depends on p53 activity. Protein lysates (100 μg) from MEF cells of passages 3 and 6 (*A*) or from different tissues of 8-month-old mice (*B*) were immunoblotted with the respective antibodies. (*C*) WT MEF cells transduced with EGFP or Cdc42F28L/EGFP were stained for β-galactosidase activity at an early passage (passage 6) to reveal the senescent cell populations. (*D*) The population doubling times of MEF cells of various genotypes at passages 4–9 were measured in cell culture. (*E*) The MEF cells at passage 7 were stained with the senescence marker SA-β-gal to determine the senescent cell populations. (*F*) A working model for a possible mechanism of Cdc42GAP deficiency-induced senescence. Cdc42GAP knockout causes a constitutively elevated Cdc42 activity, which in turn dampens the DNA damage repair ability. The accumulated genomic abnormalities resulting from the unrepaired damages stimulate a p53-mediated response that causes replicative senescence.

early onset of senescence in cells and premature aging-like phenotypes in the animal. In particular, Cdc42GAP gene targeting induces a global increase of Cdc42 activity and promotes cell genomic instability with reduced DNA damage repair ability, which in turn can activate p53 and p16^{Ink4a}, leading to early senescence (Fig. 5*F*). Previously, Cdc42 has been found to be activated in senescent cells to modulate morphological adjustment (26). It has also been proposed to be involved in p53-regulated cell morphological change, apoptosis, and proliferation (27–29) and in c-Jun N-terminal kinase-controlled apoptosis (30, 31), events that have been associated with cellular senescence and animal aging (32, 33). Our findings that Cdc42 activation is associated with natural aging and that Cdc42GAP deficiency causes a DNA damage repair defect to allow cells to accumulate genomic abnormalities that leads to early senescence further suggest a functional link between Cdc42 activity and mammalian aging.

Activation of the p53 pathway or the disruption of genes involved in DNA damage repair or genomic stability regulation has been shown to induce early aging in mice (11, 12, 33, 34). Consistent with previous observations that Cdc42 may not be involved in regulating cellular superoxide activities (17), we found that the accumulated DNA damage in Cdc42GAP$^{-/-}$ cells is not associated with the ROS activity because homozygous cells do not show increased ROS activity. Cdc42GAP deletion causes a marked reduction of DNA damage repair ability in a broad spectrum, including responses to the DNA cross-linking agent and the double-strand break or single-strand break inducer, suggesting that prolonged activation of Cdc42 may dampen DNA damage repair ability. The diversity of the genomic damage found in the Cdc42GAP$^{-/-}$ cells also is consistent with an impact from a global DNA damage repair defect. The important questions remaining to be addressed include what specific molecular determinants are involved in Cdc42GAP-regulated DNA damage repair and what upstream signal(s) causes increased Cdc42-GTP during the normal aging process.

Experimental Procedures

Mouse Breeding, Maintenance, and Longevity. Cdc42GAP$^{-/-}$ and p53$^{-/-}$ mice were generated as previously described (6, 35), and the mice used in the studies were mixed C57BL/6$^{+/-}$ 129/Sv inbred. Littermates of different genotypes were housed and fed freely with standard mouse chow over their life span in a pathogen-free environment and were monitored for vitality and longevity. Mice exhibiting extreme morbidity were euthanized and subjected to necropsy. All animal procedures were approved by the Institutional Animal Care and Use Committee at the Children's Hospital Research Foundation.

Bone Analysis. Mice were euthanized by CO_2 inhalation, and the skins were removed. After photographs were taken, the mice or dissected tibias and femurs were x-rayed further, and the bone mineral density was quantified.

Histology. Different mouse tissues were fixed in 10% neutral-buffered formalin, embedded in paraffin, divided into 5-μm-thick sections, and stained with H&E. The femurs and tibias were decalcified before sectioning.

Wound Healing Analysis. Mice were anesthetized, the dorsum was shaved, and two 5-mm-diameter punch biopsy incisions were made through the skin. Panniculus carnosus muscle and the wound healing was monitored for 4 days by measuring the distance of the healing region. Wounded skin specimens were collected 4 days after wounding and were further processed for histopathological staining.

MEF Generation and Growth Assay. Embryos from timed pregnant females were collected at embryonic days 12.5–14.5, mechanically dissociated, trypsinized, filtered through a 100-μM mesh, washed, and plated in DMEM containing 10% FBS. The proliferation capability of the cells was assessed by serial passages. MEF cells (1×10^6) were plated on day 0, and the cells were harvested, counted, and replated at the same density every 3 days for 30 consecutive days. Population-doubling for each passage was calculated by using a log2 (cells harvested per cells seeded) formula. At least three independently derived MEF clones were examined in each experiment.

β-Galactosidase Activity Assay. Senescent MEF cells were identified by their ability to stain positively for SA-β-gal (pH 6.0) as described (36). Cryosections (5-μm-thick) of mouse liver, spleen, and kidney also were stained for the SA-β-gal activity.

Karyotype Analysis. Metaphase slides were prepared from MEF cells and splenocytes (10). Slides were aged at 55°C overnight before the addition of DAPI. Metaphase spreads were captured, and images were analyzed. Reverse DAPI chromosomes were observed for aberrations. At least 50 cells for each genotype were counted and analyzed.

ROS and H_2O_2 detection. MEF cells were resuspended in prewarmed PBS buffer containing 5 μM 2,7-dichlorodihydrofluorescein diacetate. After being washed, the cells were subjected to flow cytometry analysis for the quantification of fluorescent intensity. The relative H_2O_2 concentrations in MEF cells were measured with a hydrogen peroxide colorimetric assay kit (Assay Designs, Ann Arbor, MI) by following the manufacturer's instructions.

DNA Damage Response Assay. To assay for sensitivity to DNA damage, 5×10^4 MEF cells were plated into six-well plates in triplicates overnight, and the cells were either subjected to γ-irradiation at defined doses or treated with various concentrations of H_2O_2, methyl-methane sulfonate, camptothecin, or mitomycin C for 24 h. The cells were then washed with PBS twice and grown in normal culture medium for 7 days. The survival rate of treated cells was calculated after normalization to that of nontreated cells.

We thank James F. Johnson and Clara Blair for excellent technical assistance and Drs. Qishen Pang, Paul Andreasson, James Mulloy, and Hartmut Geiger for helpful comments on the manuscript. This work was supported by National Institutes of Health Grants CA105117 and GM53943 (to Y.Z.).

1. Ridley AJ (1995) *Curr Opin Genet Dev* 5:24–30.
2. Etienne-Manneville S, Hall A (2002) *Nature* 420:629–635.
3. Cerione RA (2004) *Trends Cell Biol* 14:127–132.
4. Chen F, Ma L, Parrini MC, Mao X, Lopez M, Wu C, Marks PW, Davidson L, Kwiatkowski DJ, Kirchhausen T, *et al.* (2000) *Curr Biol* 10:758–765.
5. Moon SY, Zheng Y (2003) *Trends Cell Biol* 13:13–22.
6. Wang L, Yang L, Burns K, Kuan CY, Zheng Y (2005) *Proc Natl Acad Sci USA* 102:13484–13489.
7. Wu X, Quondamatteo F, Lefever T, Czuchra A, Meyer H, Chrostek A, Paus R, Langbein L, Brakebusch C (2006) *Genes Dev* 20:571–585.
8. Cappello S, Attardo A, Wu X, Iwasato T, Itohara S, Wilsch-Brauninger M, Eilken HM, Rieger MA, Schroeder TT, Huttner WB, *et al.* (2006) *Nat Neurosci* 9:1099–1107.
9. Chen L, Liao GH, Yang L, Cambell K, Nakafuku M, Kuan CY, Zheng, Y. (2006) *Proc Natl Acad Sci USA* 103:16520–16525.
10. Baker DJ, Jeganathan KB, Cameron JD, Thompson M, Juneja S, Kopecka A, Kumar R, Jenkins RB, de Groen PC, Roche P, *et al.* (2004) *Nat Genet* 36:744–749.
11. Maier B, Gluba W, Bernier B, Turner T, Mohammad K, Guise T, Sutherland A, Thorner M, Scrable H (2004) *Genes Dev* 18:306–319.
12. Cao L, Li W, Kim S, Brodie SG, Deng CX (2003) *Genes Dev* 17:201–213.
13. Xing Z, Ryan MA, Daria D, Nattamai KJ, Van Zant G, Wang L, Zheng Y, Geiger H (2006) *Blood* 108:2190–2197.
14. Wang L, Yang L, Filippi MD, Williams DA, Zheng Y (2006) *Blood* 107:98–105.
15. Busuttil RA, Dolle M, Campisi J, Vijga J (2004) *Ann NY Acad Sci* 1019:245–255.
16. d'Adda di Fagagna F, Reaper PM, Clay-Farrace L, Fiegler H, Carr P, Von Zglinicki T, Saretzki G, Carter NP, Jackson SP (2003) *Nature* 426:194–198.
17. Diebold BA, Fowler B, Lu J, Dinauer MC, Bokoch GM (2004) *J Biol Chem* 279:28136–28142.
18. Vogel H, Lim DS, Karsenty G, Finegold M, Hasty P (1999) *Proc Natl Acad Sci USA* 96:10770–10775.
19. Chang S, Multani AS, Cabrera NG, Naylor ML, Laud P, Lombard D, Pathak S, Guarente, L, DePinho RA (2004) *Nat Genet* 36:877–882.
20. Brown JP, Wei W, Sedivy JM (1997) *Science* 277:831–834.
21. Serrano M, Lin AW, McCurrach ME, Beach D, Lowe SW (1997) *Cell* 88:593–602.
22. Campisi J (2000) *In Vivo* 14:183–188.
23. Stewart SA, Ben-Porath I, Carey VJ, O'Connor BF, Hahn WC, Weinberg RA (2003) *Nat Genet* 33:492–496.
24. Chen Q, Fischer A, Reagan JD, Yan LJ, Ames BN (1995) *Proc Natl Acad Sci USA* 92:4337–4341.
25. Lundberg AS, Hahn WC, Gupta P, Weinberg RA (2000) *Curr Opin Cell Biol* 12:705–709.
26. Cho KA, Ryu SJ, Oh YS, Park JH, Lee JW, Kim HP, Kim KT, Jang IS, Park SC (2004) *J Biol Chem* 279:42270–42278.
27. Gadea G, Lapasset L, Gauthier-Rouviere C, Roux P (2002) *EMBO J* 21:2373–2382.
28. Guo F, Zheng Y (2004) *Mol Cell Biol* 24:1426–1438.
29. Thomas A, Giesler T, White E (2000) *Oncogene* 19:5259–5269.
30. Coso OA, Chiariello M, Yu JC, Teramoto H, Crespo P, Xu N, Miki T, Gutkind JS (1995) *Cell* 81:1137–1146.
31. Minden A, Lin A, Claret FX, Abo A, Karin M (1995) *Cell* 81:1147–1157.
32. Wang MC, Bohmann D, Jasper H (2005) *Cell* 121:115–125.
33. Tyner SD, Venkatachalam S, Choi J, Jones S, Ghebranious N, Igelmann H, Lu X, Soron G, Cooper B, Brayton C, *et al.* (2002) *Nature* 415:45–53.
34. de Boer J, Andressoo JO, de Wit J, Huijmans J, Beems RB, van Steeg H, Weeda G, van der Horst GT, van Leeuwen W, Themmen AP, *et al.* (2002) *Science* 296:1276–1279.
35. Jacks T, Remington L, Williams BO, Schmitt EM, Halachmi S, Bronson RT, Weinberg RA (1994) *Curr Biol* 4:1–7.
36. Dimri GP, Lee X, Basile G, Acosta M, Scott G, Roskelley C, Medrano EE, Linskens M, Rubelj I, Pereira-Smith O, *et al.* (1995) *Proc Natl Acad Sci USA* 92:9363–9367.